Ionics
DOI 10.1007/s11581-016-1643-z

ORIGINAL PAPER

Crystal structure analysis of Li_3PO_4 powder prepared by wet chemical reaction and solid-state reaction by using X-ray diffraction (XRD)

Nur I. P. Ayu[1] · **Evvy Kartini**[2] · **Lugas D. Prayogi**[1] · **Muhamad Faisal**[1] · **Supardi**[2]

Received: 20 February 2015 / Revised: 16 December 2015 / Accepted: 5 January 2016

Abstract Lithium phosphate (Li_3PO_4) is one of the promising solid electrolyte materials for lithium-ion battery because of its high ionic conductivity. A crystalline form of Li_3PO_4 had been prepared by two different methods. The first method was wet chemical reaction between LiOH and H_3PO_4, and the second method was solid-state reaction between Li_2O and P_2O_5. Crystal structure of Li_3PO_4 white powder had been investigated by using an X-ray diffraction (XRD) analysis. The results show that Li_3PO_4 prepared by wet chemical reaction belongs to orthorhombic unit cell of β-Li_3PO_4 with space group $Pmn2_1$. Meanwhile, Li_3PO_4 powder prepared by solid-state reaction belongs to orthorhombic unit cell of γ-Li_3PO_4 with space group Pmnb and another unknown phase of $Li_4P_2O_7$. The impurity of $Li_4P_2O_7$ was due to phase transformation in solid state reaction during quenching of molten mixture from high temperature. Ionic conductivity of Li_3PO_4 prepared by solid-state reaction was ~3.10^{-7} S/cm, which was higher than Li_3PO_4 prepared by wet chemical reaction ~4.10^{-8} S/cm. This increasing ionic conductivity may due to mixed crystal structures that increased Li-ion mobility in Li_3PO_4.

Keywords Lithium phosphate · Li_3PO_4 · X-ray diffraction · Crystal structure

✉ Nur I. P. Ayu
nurikapujiayu17@gmail.com

[1] Engineering Physics, Institut Teknologi Sepuluh Nopember, ITS Campus, Sukolilo, Surabaya 60111, Indonesia

[2] Science and Technology Center for Advanced Material, BATAN, PUSPIPTEK, Serpong, Tangerang Selatan, Banten 15314, Indonesia

Introduction

The development of Lithium-ion battery receives considerable attentions recently. Lithium-ion battery is the most famous rechargeable battery up to date, due to higher capacity, recycle ability, and environmentally friendly. In general, lithium-ion battery contains electrode, separator, and electrolyte. The electrode material must have good electronic and ionic conductivity, and the electrolyte material must have high ionic conductivity, since it serves as a lithium-ion transfer medium [1, 2]. The common electrolyte used in lithium-ion battery is liquid electrolyte, i.g., $LiPF_6$ which is a flammable material; therefore, it must be avoided from the atmosphere. A polymer separator is an isolator that normally applied between the cathode and anode to prevent the short circuit. However, this material showed very low melting point and could not be operated at temperature higher than 70 °C. As an isolator material, separator is easily getting short and causing explosion. Due to these problems, liquid electrolyte and separator should be replaced with a solid material with high ionic conductivity termed as solid electrolyte [3]. The previous research has studied super ionic conducting glasses, i.g., phosphate glasses material that could be applied as a solid electrolyte material [4–7].

This research proposed solid electrolyte material, lithium phosphate (Li_3PO_4), because of ease of preparation, low melting points, strong glass-forming character, and simple composition [8]. The ionic conductivity value of Li_3PO_4 is almost equivalent to its total conductivity value ~7×10^{-8} S/cm [9, 10]. This value is still low for the standard ionic conductivity for electrolyte that is about 10^{-3} S/cm [2]. Various methods were applied to increase the ionic conductivity of Li_3PO_4, such as doping by other compounds in various methods [11, 12].

The ionic conductivity of ceramic material is affected by crystal structure and phase. Phase transitions in the same

Published online: 25 January 2016

structure can manifest changing of the Arrhenius slope plot revealing activation energy [13]. Structure calculation and computer modeling of Li_3PO_4 phase has been done in previous research [14]. There are three polymorphs of Li_3PO_4 that stable at progressively higher temperatures: α, β, and γ-Li_3PO_4. The transition temperatures of these three polymorphs β, γ, and α- Li_3PO_4 are, respectively, about 500 °C, 1170 °C, and 1220 °C [15]. β-Li_3PO_4 is thermo-dynamically stable at the temperature under 400 °C. Although many works on the Li_3PO_4 ionic conductors have been previously reported, it is only the few papers that present complete discussion on the relationships between the synthesize method, the crystal structure and ionic conductivity. Therefore, the aim of this work was to investigate the crystal structure of Li_3PO_4 prepared two methods, namely by wet chemical reaction and by solid-state reaction.

Methodology

Lithium phosphate (Li_3PO_4) was prepared by two methods, namely wet chemical reaction and solid-state reaction. In wet chemical reaction, precursors LiOH and H_3PO_4 were reacted at 40 °C to obtain precipitation of Li_3PO_4. After filtered and rinsed, they were heated in the oven at temperature 110 °C to evaporate H_2O. The final product was white granular powders of Li_3PO_4. In order to obtain the fine powders, it was finally grounded for an hour.

The synthesis of Li_3PO_4 by solid-state reaction or melt quenching method was done by reacting Li_2O and P_2O_5 with molar ratio 3:1 [4]. The precursors of this reaction, Li_2CO_3 (99 % Alfa Aesar) and $NH_4H_2PO_4$ (99 % Merck), were mixed and grounded in a porcelain crucible. The mixture was then gradually heated up from 200 °C to 775 °C for about 2.5 h. The molten mixture was quenched into liquid nitrogen to obtain granular pieces of Li_3PO_4. The pieces of Li_3PO_4 were then grounded for an hour. The sample preparation and characterization were performed at the Integrated Battery Laboratory BATAN PUSPIPTEK, Serpong, Indonesia.

The crystal structures of Li_3PO_4 powders prepared by both methods were measured at room temperature by X-ray diffraction (XRD) of PANalytical instrument using copper at λ Kα1 1.54096 Å. The X-ray source was a conventional sealed 2500-watt X-ray tube operated at 45 kV and 40 mA. The X-ray diffraction patterns were compared with the Crystallography Open Database, then the X-ray data was analyzed by using Rietveld refinement [16] with general structure analysis system (GSAS) software. The ionic conductivities were measured by electrochemical impedance spectroscopy (EIS) in the frequency range from 42 Hz to 1.5 MHz at room temperature, and the microstructures were measured by a scanning electron microscopy (SEM). These data will be correlated with the crystal structure of Li_3PO_4 solid electrolyte.

Results and discussion

The main purpose of this research was to investigate the crystal structure of Li_3PO_4 obtained from different synthesis methods, wet chemical reaction, and solid-state reaction. According to Popovic, the β to γ transition was occurred above 580 °C [15]. The wet chemical reaction occurred at a relatively low temperature, while the solid-state reaction occurred at high temperature above the melting point of the precursor.

In our study, the crystal structure results were obtained from the refinement of X-ray diffraction (XRD) data. Firstly, the data was compared with the diffraction pattern database of Crystallography Open Database (COD) to get the crystal structure models. Then, the data was refined by Rietveld refinement. The refined parameters were lattice parameters, atom coordinates, and temperature factor (isotropic).

XRD pattern of Li_3PO_4 powder obtained by wet chemical reaction matched with COD 901-2501, lithium phosphate orthorhombic with space group $Pmn2_1$. The broad peaks may indicate the small crystallite size, as can be seen in Fig. 1. Furthermore, the Rietveld refinement using GSAS software was done to investigate the crystal structure of Li_3PO_4 sample. The crystal structure model used in this work was COD 901-2500. The refinement results at $\chi^2 = 2.09$, Rp = 0.055, and Rwp = 0.042, represented that Li_3PO_4 was in orthorhombic crystal structure (symmetry $Pmn2_1$ #31) with lattice parameters a = 6.1295(2) Å, b = 5.2546(2) Å, and c = 4.8705(1) Å. This lattice parameter values were close to the lattice parameters of β-Li_3PO_4 phase obtained by Holzwart in a previous research [17]. Therefore, Li_3PO_4 prepared by wet chemical reaction belongs to β-Li_3PO_4 phase. The low temperature phase of Li_3PO_4 [18, 19] was formed due to low temperature condition of the wet chemical reaction.

The Rietveld refinement pattern of Li_3PO_4 powder prepared by solid-state reaction identified that the synthesized powder was contained by three phases, namely γ-Li_3PO_4, β-Li_3PO_4, and $Li_4P_2O_7$. The narrow peaks, as shown in Fig. 2, indicate the bigger crystallite size than that of wet chemical reaction results. The crystallite size of Li_3PO_4 powder of solid-state reaction calculated from FWHM using Debyee Scherer equation is about 762 Å; this value is higher than those of wet chemical reaction results ~478 Å. The γ-Li_3PO_4, β-Li_3PO_4, and $Li_4P_2O_7$ patterns respectively referred to COD 901-282, COD 901-2500, and Holzwarth model [17]. The X-ray diffraction pattern refinement result of the powder prepared by solid-state reaction at $\chi^2 = 2.22$, Rp = 0.041, and Rwp = 0.0546 indicated that the powder highly dominated by γ-Li_3PO_4 (approximately about ~88.15 %) with orthorhombic structure Pmnb (62). The lattice parameters of γ-Li_3PO_4 obtained from this analysis were a = 6.1149(0) Å, b = 10.4728(2) Å, and c = 4.9238(0) Å. The lattice parameter was close to γ-Li_3PO_4 prepared by Yiu and Yaojun [20, 21] as presented in Table 1. The high-temperature phase of Li_3PO_4

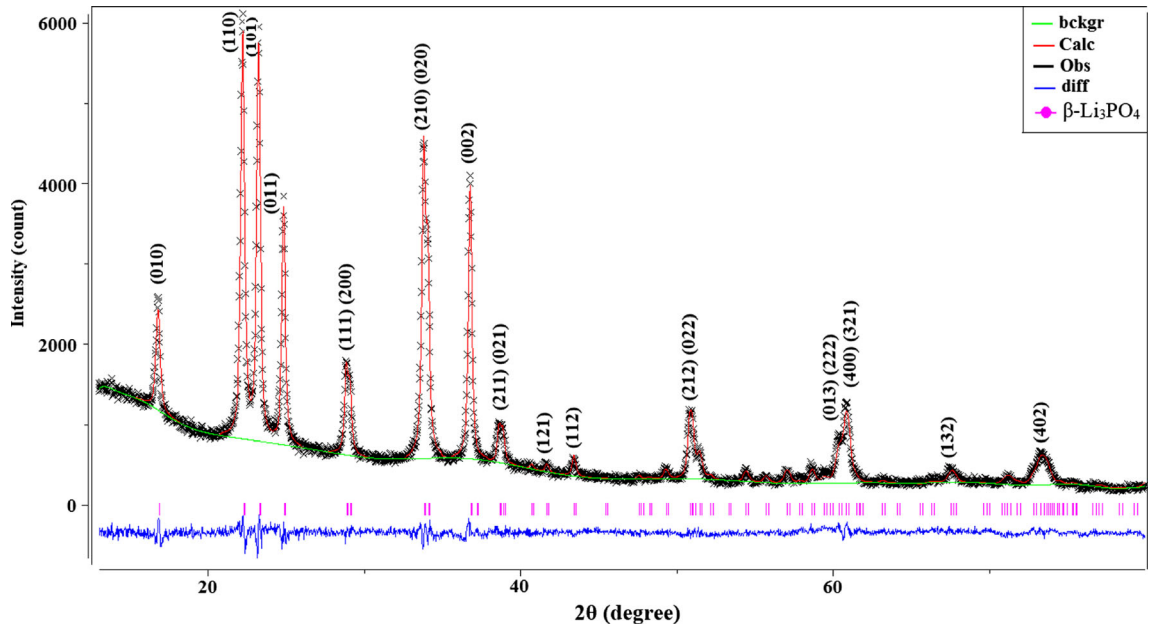

Fig. 1 X-ray diffraction pattern of Li_3PO_4 prepared by wet chemical reaction

formation was in good agreement with the high-temperature condition of solid-state reaction up to 775 °C that was higher than transition temperature of β to γ [15].

In the structure of β-Li_3PO_4 Li and P were in tetrahedral sites, and all tetrahedral sharing vertices point to the same direction [18]. With reference to the face-centered, all octahedral sites were unoccupied while tetrahedral sites were occupied. On the other hand, the oxygen of β- or γ-Li_3PO_4 was shared by three LiO_4 tetrahedral. The LiO_4 tetrahedral shares vertices with PO_4 tetrahedral. A major difference between the β and γ structures was that in β-Li_3PO_4, only vertex sharing existed, but in γ-Li_3PO_4, some edge sharing of LiO_4 occurred [12]. The atom coordinate of Li_3PO_4 from this work is listed in Table 2. Both polymorphs, β- and γ-Li_3PO_4 have the orthorhombic crystal structure; the structures are presented in Fig. 3. While β phase was heated up, the atom vibration may contribute to the bond strength changing. During the heating treatment from

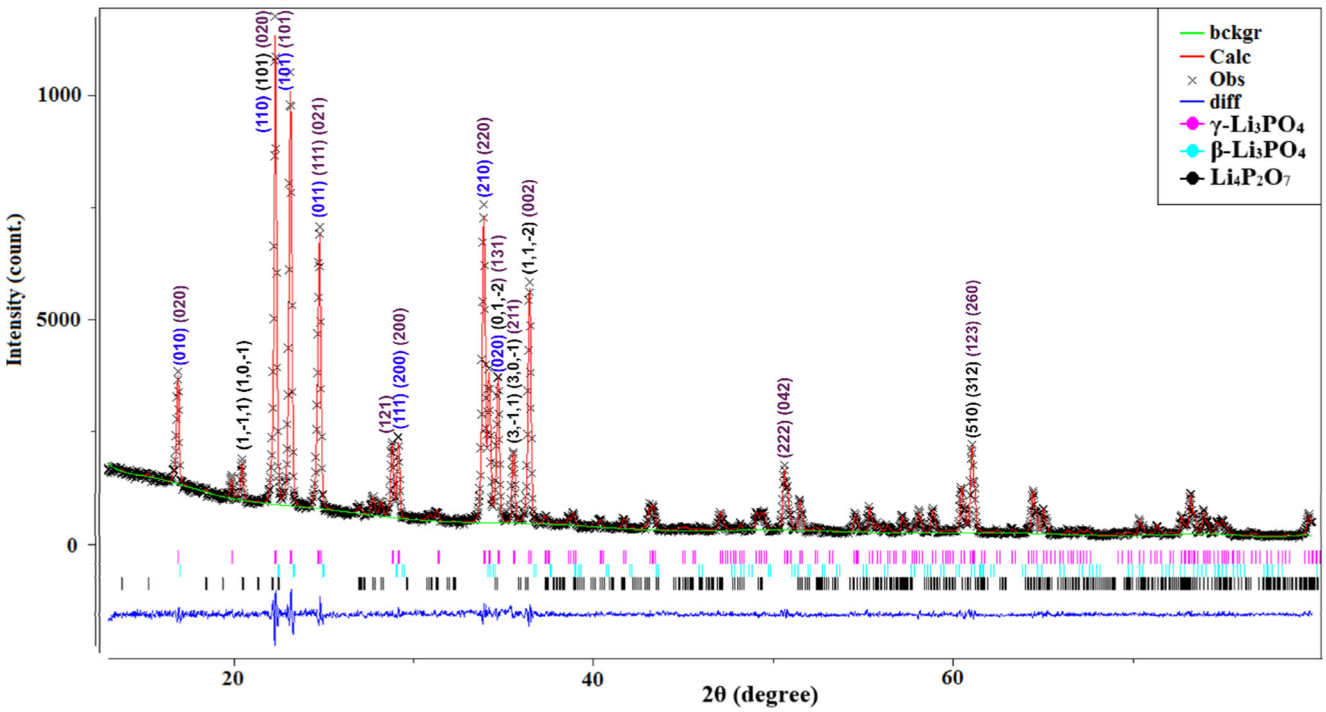

Fig. 2 X-ray diffraction pattern of Li_3PO_4 prepared by solid state reaction

Table 1 Crystal parameters of Li_3PO_4 in comparison with the other works

	a (Å)	*b* (Å)	*c* (Å)
β-Li_3PO_4			
Ref. 17	6.12	5.24	4.86
This work (wet chemical)	6.1295(2)	5.2546(2)	4.8705(1)
γ-Li_3PO_4			
Ref. 21	6.17	10.58	4.99
Ref. 20	6.1113	10.4612	4.9208
This work (solid-state)	6.1149(0)	10.4728(2)	4.9238(0)

200 °C up to 775 °C, the bond strength changing was commonly followed by the bond length changing [15] and structure expansion. This treatment not only transforms the phase but also expands the structure in b direction. This seems to imply the β-Li_3PO_4 expansion that caused γ-Li_3PO_4 formation.

Another phase indicated as impurities, $Li_4P_2O_7$, was monoclinic with symmetry of P21/n (14). The monoclinic structure is a high-temperature phase of $Li_4P_2O_7$ [22]. As seen in Fig. 4, the monoclinic structure looks like distorted orthorhombic; hence, the high peaks of $Li_4P_2O_7$ pattern are in the same position with those of Li_3PO_4. The $Li_4P_2O_7$ formation in the solid-state reaction was due to the inhomogeneous mixing powder during grounding and quenching. This reason was revealed by Evvy Kartini in the previous research about the various results of Li_2O and P_2O_5 reaction in the various molar ratios [4]. The $Li_4P_2O_7$ would form in the same precursors with the molar ratio of 4:1. The inhomogeneous mixing influenced the powder distribution; therefore, there was a small possibility for the $Li_4P_2O_7$ formation. The percentage of the $Li_4P_2O_7$ calculated from refinement results was only about 5.38 %.

The microstructure analysis by using SEM JEOL JEM 6510LA was done. The powders with different synthesis

Table 2 Atom coordinates of Li_3PO_4 prepared by wet chemical reaction and solid-state reaction

	Mult	Sym.	*X*	*Y*	*Z*	Uiso
β-Li_3PO_4 (wet chemical reaction)						
Li	4	1	0.2473(13)	0.3270(18)	1.0128(30)	0
Li	2	M(100)	0.5000	0.8240(29)	0.9861(83)	0.0364(67)
P	2	M(100)	0.0000	0.8262(4)	−0.0096(7)	0.0034(12)
O	4	1	0.2069(5)	0.6849(6)	0.9027(9)	0.0038(20)
O	2	M(100)	0.0000	0.1104(10)	0.8959(13)	0.0022(16)
O	2	M(100)	0.5000	0.1852(8)	0.8131(7)	0
γ-Li_3PO_4 (solid-state reaction)						
Li	8	1	0.5004(10)	0.1653(6)	0.3107(15)	0.0192(25)
Li	4	M(100)	0.7500	0.4175(9)	0.2106(23)	0.0330(38)
P	4	M(100)	0.2500	0.4104(1)	0.3086(3)	0.0126(8)
O	8	1	0.0400(3)	0.3389(2)	0.2043(5)	0.0133(11)
O	4	M(100)	0.2500	0.0531(3)	0.2960(7)	0.0067(12)
O	4	M(100)	0.7500	0.0908(3)	0.1273(6)	0.0049(13)

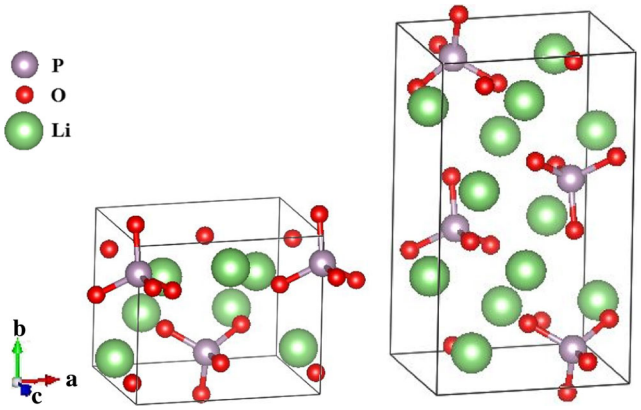

Fig. 3 Crystal structure of β-Li_3PO_4 (*left*) and γ-Li_3PO_4 (*right*)

methods have different microstructures, because it consists of different compounds. Each compound likely has its microstructure form. The microstructure of the powder prepared by wet chemical reaction showed different granule forms compared with the solid-state reaction result as shown in Fig. 5. The particle size of the powder obtained by wet chemical reaction was considerably smaller and distributed better (quite homogeny) than that of solid-state reaction, within the particle and agglomerate sizes approximately about 0.834–7.81 μm for wet chemical reaction and 2.15–17.3 μm for solid-state reaction. This homogeneity is due to almost pure ß-Li_3PO_4 phase content in the powder prepared by wet chemical reaction method. On the other hand, the microstructure of the powder obtained by solid-state reaction tends to be inhomogeneous due to the mixture compounds and phases. The big agglomerates appeared in Fig. 3b apparently consist of small particles of $Li_4P_2O_7$, since agglomeration process strongly affected by particle size; therefore, there is a strong possibility that the particle composing this big agglomerates dominated by $Li_4P_2O_7$. The agglomeration could be due to the electrostatic force in the ceramic materials. It should, however, be noted that the grounding and handling processes may affect the results.

In the energy-dispersive X-ray (EDX) pattern, Fig. 3 (a), the sampling area notated by 002 consists of P and O atom

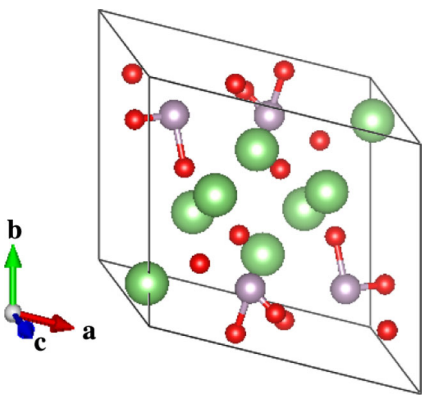

Lattice constant:
a= 8.564(3) Å
b= 7.108(2) Å
c= 5.182(1) Å

α= 111.53(3) Å
β= 89.99(2) Å
γ= 103.00(3) Å

Fig. 4 Crystal structure of $Li_4P_2O_7$. The Li, P, and O are depicted respectively with *green*, *violet*, and *red balls*

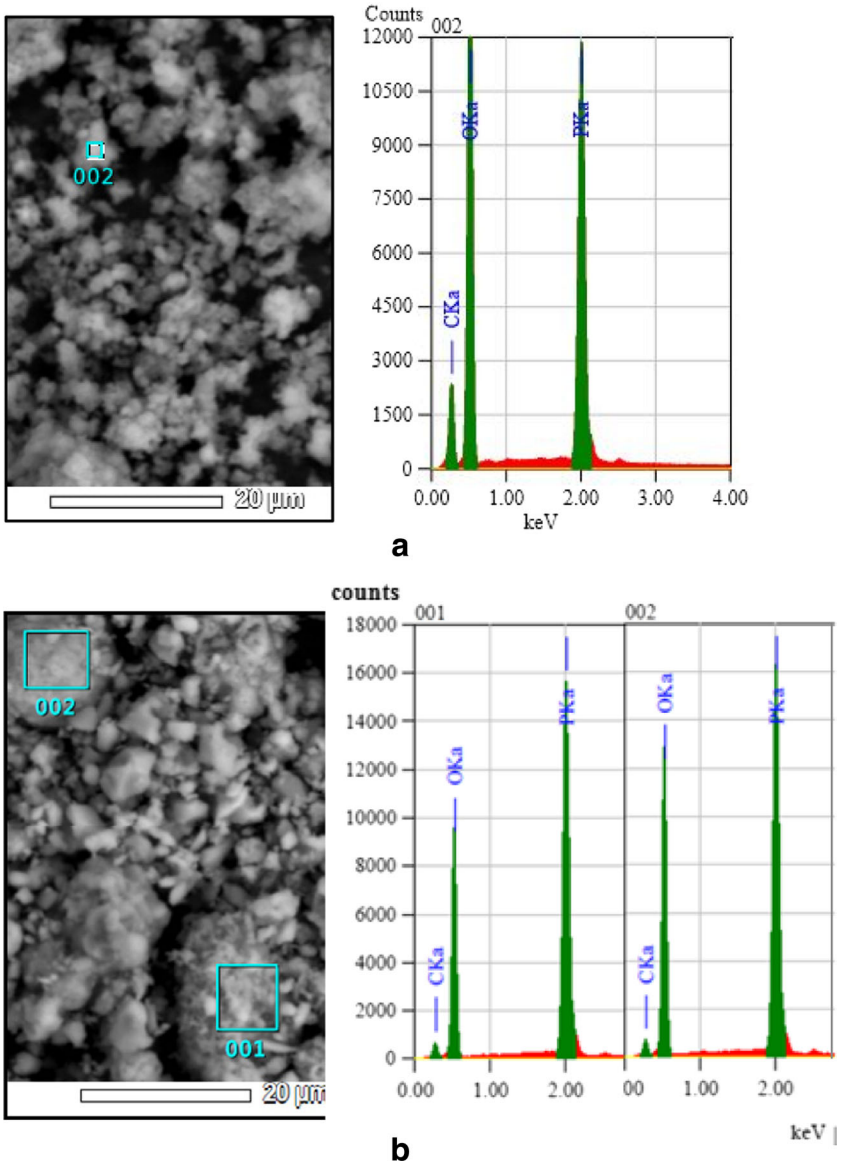

Fig 5 Microstructure analysis using SEM-EDX of **a** the wet chemical result and **b** the solid-state reaction

ratio that is close to that of Li_3PO_4. Hence, the particles can be identified as Li_3PO_4. However, the sampling areas notated 001 and 002 shown in Fig. 3 (b) gave slight difference of EDX counts for O and P ratio that was indicated as $Li_3PO_4 + Li_4P_2O_7$ mixture. The count difference of P and O atoms as shown in the EDX (Fig. 3 (b)) can be caused by bounded O and C, since C element is usually present and potentially bond with oxygen. In this analysis, the Li spectrum does not appear since Li is light atom, the lithium X-ray energy is small, and it appears that almost all energy has been absorbed by the detector cover.

The conductivity spectra in Fig. 6 indicate the slight different conductivity results of the powder obtained from wet chemical reaction and solid-state reaction. Li_3PO_4 prepared by solid-state reaction has higher conductivity than the sample prepared by wet chemical reaction. The value of conductivity can be approached by fitting the curve above. The equation used to model this graph is $\sigma \gg f^s$ with σ and s respectively represent conductivity and power exponent ($0 < s < 1$). The value of s is limited to 1 based on the many crystal observations of ionic crystal or silica glass. For supersonic conducting glass, the equation is expressed as

$$\sigma = \sigma^0 f^s \tag{1}$$

where the power of s has been influenced by the temperature to limit 1. To simplify the equation, it is linearized by writing it in the form of logarithmic function as Eq. (2) below.

$$\log\sigma = \log\sigma^0 + s\log f \tag{2}$$

where $\log \sigma^0$ is the conductivity in frequency 1 Hz.

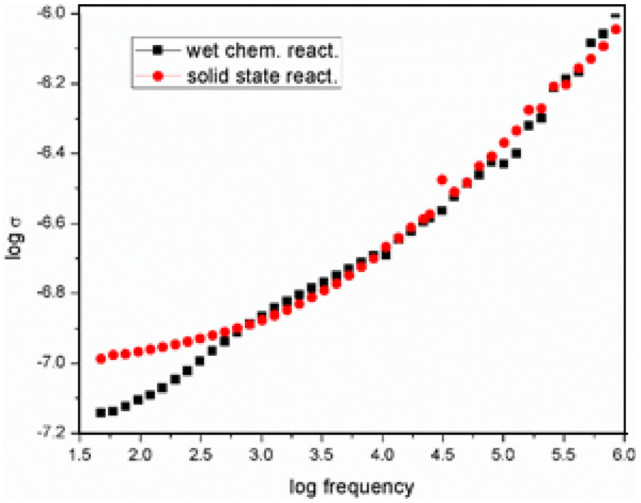

Fig 6 Frequency dependence of conductivity spectra of the powder obtained from wet chemical and solid-state reactions

The result of conductivity measurement of Li_3PO_4 can be divided into three regions of frequency, the region of low log *f* value (ionic hoping), region of medium log *f* value (plateau), and high frequency (ionic vibration) [4]. In the graph of Li_3PO_4 conductivity, region of low frequency value cannot be detected because of the limitation of measurement device. To fit the curve, it was divided only by two regions of frequency as given in Table 3.

Based on Table 3, the dc conductivity can be determined from the lowest value of *s*, which means the dependence of frequency is the lowest at that region. The value of dc conductivity for wet chemical reaction is 4.10^{-8} S/cm, and the value of dc conductivity for solid-state reaction 3.10^{-7} S/cm. The results obtained are quite different from the reference about 10^{-9} S/cm [4].

As solid electrolyte, Li_3PO_4 has a role as Li-ion transport medium. Li-ion movement in the material through two mechanisms, vacancy and intercalation [23], is influenced by the crystal structure [24]. Therefore, the crystal structure of Li_3PO_4 strongly affects the Li-ion movement that implies the ionic conductivity of Li_3PO_4. As modeled by Holzwarth and coworker, the activation energy for Li-ion migration in β-Li_3PO_4 is to be E_A = 1.4–1.6 eV [25] and in γ-Li_3PO_4 to be E_A = 1.0–1.2 eV [21]. It seems to imply that γ-Li_3PO_4 should have higher ionic conductivity than β-Li_3PO_4. Mixed crystal structure may also affect the increasing mobility of Li-ion transport in the powder prepared by solid-state reaction [24].

Table 3 Conductivity spectra fitting of Li_3PO_4 powder prepared by solid-state reaction as the function of frequency

Log *f*	Log σ^0	*s*
Wet chemical		
1.6–2.6	−7.49 (2)	0.192 (7)
2.6–6.0	−7.76 (3)	0.279 (6)
Solid-state		
1.6–2.6	−7.23 (0)	0.080 (1)
2.6–6.0	−7.86 (2)	0.288 (4)

These reasons explain the higher ionic conductivity of powder prepared by solid-state reaction.

Conclusion

Different crystalline forms of Li_3PO_4 have been prepared by two different methods, wet chemical reaction and solid-state reaction. The crystal structure of Li_3PO_4 white powder was investigated by using an X-ray diffraction (XRD) analysis. The results showed that the Li_3PO_4 prepared by wet chemical reaction belongs to orthorhombic unit cell of β-Li_3PO_4 $Pmn2_1$ (31) with lattice parameters a = 6.129, b = 5.254 and c = 4.870. While, the Li_3PO_4 powder prepared by solid-state reaction is orthorhombic unit cell of γ-Li_3PO_4 Pmnb (62) with higher b and c lattice parameter ~ a = 6.115, b = 10.472, c = 4.923 and another phase of $Li_4P_2O_7$ monoclinic structure P21/n (14). The impurity of $Li_4P_2O_7$ due to phase transformation during quenching may increase the ionic conductivity of Li_3PO_4 prepared by the solid-state reaction ~3.10^{-7} S/cm that is higher than Li_3PO_4 prepared by wet chemical reaction ~4.10^{-8} S/cm.

Acknowledgments The authors would like to thank the Ministry of Research and Technology, Indonesia, for funding this research and the Science and Technology Center for Advance Material, National Nuclear Energy Agency for the facilities supporting this research.

References

1. Whittingham MS (2004) Lithium batteries and cathode materials. Chem Rev 104:4271–4302. doi:10.1021/cr020731c
2. Linden D, Reddy TB (2001) Handbook of batteries. Third Edit. doi:10.1016/0378-7753(86)80059-3
3. Minami T, Tatsumisago M, Wakihara M, et al. (2005) Solid state ionics for batteries. Chem &amp. doi:10.1007/4-431-27714-5
4. Kartini E, Honggowiranto W, Jodi H, Jahya AK (2014) Synthesis and characterization of new solid electrolyte layer (Li_2O) 2 (P_2O_5) Y *. 14th Asian Conf. Solid State Ionics (2):978–981. doi:10.3850/978-981-09-1137-9
5. Kartini E, Nakamura M, Arai M, et al. (2014) Structure and dynamics of solid electrolyte LiI-LIPO 3 Thu-B1-05. Solid State Ionics 262:833–836. doi:10.1016/j.ssi.2013.12.041
6. Kartini E, Kennedy SJ, Itoh K, et al. (2004) Anion effect on the structure of Ag_2S-$AgPO_3$ superionic glasses. Solid State Ionics 167:65–71. doi:10.1016/j.ssi.2003.12.021
7. Kartini E, Sakuma T, Basar K, Ihsan M (2008) Mixed cation effect on silver-lithium solid electrolyte (AgI) 0.5($LiPO_3$)0.5. Solid State Ionics 179:706–711. doi:10.1016/j.ssi.2008.04.015
8. Martin SW (1991) Ionic conduction in phosphate glasses. J Am Ceram Soc 84:1767–1783. doi:10.1111/j.1151-2916.1991.tb07788.x
9. Lee C, Dutta PK, Ramamoorthy R, SA A (2006) Mixed ionic and electronic conduction in Li_3PO_4 electrolyte for a CO_2 gas sensor. J Electrochem Soc 153:H4. doi:10.1149/1.2129180
10. Takada K (2013) Progress and prospective of solid-state lithium batteries. Acta Mater 61:759–770. doi:10.1016/j.actamat.2012.10.034
11. Muñoz F, Durán A, Pascual L, et al. (2008) Increased electrical conductivity of LiPON glasses produced by ammonolysis. Solid State Ionics 179:574–579. doi:10.1016/j.ssi.2008.04.004

12. Rabaâ H, Hoffmann R, Cruz Hernández N, Fernandez Sanz J (2001) Theoretical approach to ionic conductivity in phosphorus oxynitride compounds. J Solid State Chem 161:73–79. doi:10.1006/jssc.2001.9269
13. Avdeev M, Nalbandyan VB, Shukaev IL (2009) Alkali metal cation and proton conductors: relationships between composition, crystal structure, and properties. Solid State Electrochem I Fundam Mater Their Appl. doi:10.1002/9783527627868.ch7
14. NAW H, ND L, YA D (2011) Computer modeling of lithium phosphate and thiophosphate electrolyte materials. J Power Sources 196:6870–6876. doi:10.1016/j.jpowsour.2010.08.042
15. Popović L, Manoun B, De Waal D, et al. (2003) Raman spectroscopic study of phase transitions in Li_3PO_4. J Raman Spectrosc 34:77–83. doi:10.1002/jrs.954
16. Cox DE (1994) edited by R. A. Young. J Appl Crystallogr 27:440–441. doi:10.1107/S0021889894000439
17. Lepley N, Holzwarth NAW Computer modeling of crystalline electrolytes—lithium thiophosphates and phophosphates a solid vs liquid electrolytes in Li ion batteries. 1–19.
18. AR W, FP G (1972) Preparation and crystal chemistry of some tetrahedral L & PO, −type compounds. J Solid State Chem 28:20–28. doi:10.1016/0022-4596(72)90127.2
19. Ibarra-Ramírez C, Villafuerte-Castrejón ME, AR W (1985) Continuous, martensitic nature of the transition ß → γ Li3PO4. J Mater Sci 20:812–816. doi:10.1007/BF00585719
20. Yiu YM, Yang S, Wang D, et al. (2013) Ab-initio calculation of the XANES of lithium phosphates and $LiFePO_4$. J Phys Conf Ser 430:012014. doi:10.1088/1742-6596/430/1/012014
21. Du YA, Holzwarth NAW (2007) Li ion diffusion mechanisms in the crystalline electrolyte gamma-Li_3PO_4. J Electrochem Soc 154:A999–A1004. doi:10.1149/1.2772200
22. Voronin VI, Sherstobitova EA, Blatov VA, Shekhtman GS (2014) Lithium-cation conductivity and crystal structure of lithium diphosphate. J Solid State Chem 211:170–175. doi:10.1016/j.jssc.2013.12.015
23. Adams S, Rao RP (2009) Transport pathways for mobile ions in disordered solids from the analysis of energy-scaled bond-valence mismatch landscapes. Phys Chem Chem Phys 11:3210–3216. doi:10.1039/b901753d
24. AK I-S, VV K, Mel'nikov O (2001) Growth and ionic conductivity of γ-Li_3PO_4. Crystallogr Reports 46:938–941
25. Lepley ND, NAW H, YA D (2013) Structures, Li^+ mobilities, and interfacial properties of solid electrolytes Li_3PS_4 and Li_3PO_4 from first principles. Phys Rev B 88:104103. doi:10.1103/PhysRevB.88.104103